Biomatter 3:2, e24791; April/May/June 2013; © 2013 Landes Bioscience

Kinetics and isotherm of fibronectin adsorption to three-dimensional porous chitosan scaffolds explored by ^{125}I-radiolabelling

Isabel F. Amaral,[1,*] Susana R. Sousa,[1,2] Ismael Neiva,[1] Lara Marcos-Silva,[3] Charles J. Kirkpatrick,[4] Mário A. Barbosa[1,5] and Ana P. Pêgo[1,5]

[1]INEB—Instituto de Engenharia Biomédica; Universidade do Porto; Porto, Portugal; [2]REQUIMTE; Instituto Superior de Engenharia do Porto; Instituto Politécnico do Porto; Porto, Portugal; [3]IPATIMUP—Institute of Molecular Pathology and Immunology of the University of Porto; Porto, Portugal; [4]REPAIR Lab, Institute of Pathology; University Medical Center; Johannes Gutenberg University; Mainz, Germany; [5]Universidade do Porto; Instituto de Ciências Biomédicas Abel Salazar and Faculdade de Engenharia; Porto, Portugal

Keywords: protein adsorption, protein conformation, fibronectin, fluorescence, 3-D scaffolds

In this study, ^{125}I-radiolabelling was explored to follow the kinetics and isotherm of fibronectin (FN) adsorption to porous polymeric scaffolds, as well as to assess the elution and exchangeability of pre-adsorbed FN following incubation in serum-containing culture medium. Chitosan (CH) porous scaffolds with two different degrees of acetylation (DA 4% and 15%) were incubated in FN solutions with concentrations ranging from 5 to 50 μg/mL. The kinetic and isotherm of FN adsorption to CH were successfully followed using ^{125}I-FN as a tracer molecule. While on DA 4% the levels of adsorbed FN increased linearly with FN solution concentration, on DA 15% a saturation plateau was attained, and FN adsorbed amounts were significantly lower. These findings were supported by immunofluorescent studies that revealed, for the same FN solution concentration, higher levels of exposed cell-binding domains on DA 4% as compared with DA 15%. Following incubation in serum containing medium, DA 4% also revealed higher ability to exchange pre-adsorbed FN by new FN molecules from serum than DA 15%. In accordance, when assessing the efficacy of passively adsorbed FN to promote endothelial cell (EC) adhesion to CH, ECs were found to adhere at higher levels to DA 4% as compared with DA 15%, 5 μg/mL of FN being already efficient in promoting cell adhesion and cytoskeletal organization on CH with DA 4%. Taken together the results show that protein radiolabelling can be used as an effective tool to study protein adsorption to porous polymeric scaffolds, both from single and complex protein solutions.

Introduction

Protein adsorption has an important role in modulating cell response to biomaterials. The type, amount, distribution, binding strength, and conformation of proteins adsorbed from single protein solutions, plasma, or culture medium depend on the physicochemical characteristics of the underlying substrate and ultimately determine the cell response to biomaterial surfaces.[1] In this context, protein adsorption to biomaterials is often evaluated in order to predict and better understand cell behavior on biomaterials.[2,3] In the case of anchorage-dependent cells, protein adsorption studies involving cell-adhesive proteins such as fibronectin (FN) or laminin are particularly useful to predict and explain cell response to biomaterials, such as cell adhesion and cytoskeletal reorganization, as well as other cellular events triggered by integrin signaling.

Although protein adsorption onto biomaterial surfaces has been assessed using a wide range of techniques, the quantification of protein adsorption onto porous scaffolds is still a challenging and controversial issue, namely due to the difficulty in distinguishing adsorbed from non-adsorbed protein present in the inner part of the scaffolds. With the emergence of tissue engineering and the increasing need of three-dimensional (3-D) porous scaffolds, protocols for the quantitative assessment of protein adsorption to porous scaffolds need to be established. **Table 1** provides an overview of the main methodologies that have been used for the quantitative analysis of protein adsorption to porous biomaterials. Their main advantages and limitations are briefly described.

Radiolabelling is considered the gold standard of the methodologies available to follow protein adsorption, as it is a straightforward and sensitive quantitative technique. Iodine radioisotopes are usually used, as iodine readily binds to the tyrosine residues of proteins and the signals emitted are directly proportional to protein amount.[2] ^{125}I-radiolabelling can be used to quantify protein adsorption from single protein solutions or from complex mixtures of proteins, such as serum-containing media and blood plasma.[2] The retention, desorption, as well as the exchangeability

*Correspondence to: Isabel F. Amaral; Email: iamaral@ineb.up.pt
Submitted: 12/20/12; Revised: 03/15/13; Accepted: 04/24/13
Citation: Amaral I, Sousa S, Neiva I, Marcus-Silva L, Kirkpatrick C, Barbosa M, Pêgo A. Kinetics and isotherm of fibronectin adsorption to three-dimensional porous chitosan scaffolds explored by ^{125}I-radiolabelling. Biomatter 2013; 3:e24791;; http://dx.doi.org/10.4161/biomatter.24791

of the adsorbed protein by other proteins can also be easily determined, which makes radiolabelling a powerful tool to provide insights into protein adsorption phenomena occurring at the interface of biomaterials with the biological milieu.[4,5] This sensitive technique has been widely explored to follow protein adsorption onto polymeric surfaces.[6,7] Nevertheless, only a few authors have used this technique to measure protein adsorption onto porous scaffolds.

In an attempt to develop a pre-vascularized scaffold for use in cell-based regenerative therapies, we have shown that the endothelialisation of chitosan porous scaffolds could be successfully achieved by prior incubation of the porous matrices in a 40 μg/mL FN solution. In that study physiadsorption of FN was shown to be effective in promoting endothelial (EC) adhesion and proliferation on CH scaffolds with retention of the EC phenotype and angiogenic ability.[8] However, the effectiveness of the FN treatment was found to be dependent on the degree of acetylation (DA) of CH, a parameter influencing directly CH susceptibility to enzymatic degradation, in vivo.[9] In the present work we assessed the effect of FN concentration on CH ability to promote cell adhesion and cytoskeletal organization of ECs. Scaffolds with two different DAs, namely DA 4% and DA 15%, were evaluated. While the former are less susceptible to enzymatic degradation (DA 4%), the latter are expected to degrade faster. As a result, both may be of interest for tissue engineering, depending of the final application. To determine the kinetics and isotherm of FN adsorption to CH scaffolds, as well as the elution and exchangeability of pre-adsorbed FN in the presence of serum proteins, ^{125}I-radiolabelling was explored. To evaluate FN conformation following adsorption to CH, immunofluorescent detection of cell-binding domains was performed. The results provided by the two different techniques were then correlated with EC behavior on FN-coated CH porous scaffolds.

Results

Characterization of CH 3-D porous scaffolds. SEM analysis of cross-sectional areas of CH scaffolds revealed a highly porous and homogeneous structure with interconnected macropores with average diameter in the range of 100 to 120 μm for both the DAs used, and in line with previous results (**Fig. 1A**).[8] Scaffold analysis by mercury intrusion porosimetry revealed for DA 4% a lower surface area as compared with DA 15%, namely of 45.8 m^2/g and 87.4 m^2/g, respectively. Further characterization of CH scaffolds in the hydrated state showed a similar structure for both the DAs (**Fig. 1B**). Subsequent image analysis revealed, for both the DAs, a pore size distribution in the range of 23 to 120 μm, due to the contribution of the small round-shaped pores present in the thin walls of the scaffolds which are responsible for interconnectivity (**Fig. 1B**). No statistically significant differences in terms of pore size were found between the two types of scaffolds.

Fibronectin (FN) adsorption to CH scaffolds and elution/exchangeability of adsorbed FN upon incubation in complete culture medium (CCM). Protein adsorption studies revealed similar FN adsorption to CH scaffolds, regardless of the ratio ^{125}I-FN/FN used (2–20%), indicating that preferential adsorption of ^{125}I-FN does not occur (**Fig. S1**). Kinetic studies performed over a 12 h period showed a steep increase of FN adsorption during the first 3 h of incubation (**Fig. 2A**). After this time point, FN adsorption showed evidence of beginning to level off. Although the levels of adsorbed FN increased with incubation time after 3 h of incubation, these were not found to be statistically significantly different. The isotherm of FN adsorption to CH matrices with DA 4% revealed an increase of FN adsorption with increasing FN concentration (**Fig. 2B**). Matrices with DA 15% showed a similar trend for FN concentrations up to 30 μg/mL, attaining then a plateau. However, for all the FN concentrations tested, significantly lower amounts of FN were found for DA 15% scaffolds. In fact, for most of the FN concentrations tested, namely 5, 10, 20, 30 and 50 μg/mL, the levels of FN found for DA 15% were in the range of two to 3-fold lower than those of DA 4%. The elution and the exchangeability of pre-adsorbed FN following incubation in CCM were investigated in CH scaffolds previously incubated in a 20 μg/mL FN solution (**Fig. 3**). Prior to incubation in CCM, levels of adsorbed FN of 0.15 (± 0.01) and 0.07 (± 0.01) μg/mg of CH scaffold were found for DA 4 and 15%, respectively. As expected, partial elution of pre-adsorbed FN occurred following subsequent incubation with competitive proteins, as shown by the levels of FN found after incubation in CCM for 24 h, namely of approx. 0.10 and 0.05 μg/mg of scaffold for DA 4 and 15%, respectively. The release of pre-adsorbed FN was similar between the two types of scaffolds: while DA 4% scaffolds eluted 36% (± 7.6%) of the initial adsorbed FN, DA 15% scaffolds eluted about 32% (± 18%). When comparing the ability of the two FN-coated scaffolds to adsorb new FN molecules from CCM, DA 4% scaffolds were found to adsorb higher amounts than DA 15% (app. 3.7-fold higher, $p = 0.001$). To estimate the exchangeability of pre-adsorbed FN during the immersion step in CCM, the levels of eluted FN were compared with those correspondent to new FN molecules adsorbed from CCM. While DA 4% were able to exchange all eluted FN (119%), DA 15% were able to exchange only 85% of eluted FN. Finally, the ability of bare CH scaffolds to adsorb FN from CCM was assessed. The correspondent results are shown in **Figure S2** of the supporting data. Once again, significantly higher FN adsorption levels (app. 2-fold higher, $p = 0.004$) were found for DA 4% as compared with DA 15%. These levels were compared with those reached incubating the scaffolds in a single FN solution prepared at a concentration such as to provide the same amount of FN present in the CCM used (app. 40 μg/mL).[10] For both scaffolds, results show that FN adsorption from CCM was in the range of 14 to 16% of the amount adsorbed from a 40 μg/mL FN solution, which reflects well the influence of competitive proteins from serum on FN adsorption.

FN exposure of cell-binding domains upon adsorption to CH scaffolds. The distribution and conformation of FN upon adsorption were examined by immunofluorescent labeling of FN cell-binding domains in 100 μm thick cross-sections. CLSM imaging showed a very faint labeling for FN on scaffolds incubated in CCM, regardless of the DA (**Fig. S3**). In contrast, incubation in a 20 μg/mL FN solution resulted in a homogeneous

Table 1. Methodologies used for the quantitative analysis of protein adsorption in porous biomaterials

Method	Principle	Information provided	Main advantages	Main limitations*	Reference
Solution depletion method	Protein concentration is measured in protein solution prior to and after adsorption using one of the following techniques: electrophoresis, colorimetry, UV absorption, as well as use of fluorescently or radioisotope-labeled proteins.	• Protein adsorption. • Competitive adsorption, if fluorescently or radioisotope-labeled proteins are used.	• Simplicity.	• Indirect method. • Requires additional analysis of protein levels in the rinsing solutions to estimate the contribution of non-adsorbed protein to the amount of depleted protein.	31–33
Bicinchoninic acid (BCA) method	Desorbed protein is quantified colorimetrically based on protein ability to reduce Cu^{+2} to Cu^{+1} in an alkaline medium in the presence of BCA.	• Protein adsorption.	• Simplicity.	• Indirect method, since protein desorption is required. • Adsorbed amount may be underestimated. • Calibration is required.	34, 35
Fluorescence	Following sample incubation with fluorescently-labeled proteins, protein is desorbed with a surfactant detergent and subsequently quantified using a fluorescence spectrometer.	• Protein adsorption. • Protein adsorption in the presence of competitive proteins (competitive adsorption). • Distribution/organization of the protein layer.	• Simplicity. • May be used to assess protein distribution.	• Indirect method, since protein desorption is required. • Adsorbed amount may be underestimated. • Calibration is required.	36, 37
Aminoacid analysis	Following sample dissolution protein is hydrolyzed with hot acid and then lyophilized. The hydrolysed samples are then analyzed using an amino acid analyzer (i.e., ion exchange separation of the amino acids followed by post column detection with ninhydrin).	• Protein adsorption.	• Accuracy.	• Not applicable for scaffolds containing protein in their composition. • Sample dissolution is required. • Analysis requires at least 20 μg of protein.	38[§]
Protein radiolabelling	Following sample incubation with radioisotope-labeled proteins the amount of adsorbed protein is detected by radioisotope counting.	• Protein adsorption. • Protein adsorption in the presence of competitive proteins (competitive adsorption).	• Direct method. • Simplicity. • Highly sensitive.	• Requires expensive support equipment and, in certain countries, special licensing.	8, 39

*Regardless of the methodology used, the use of multiple rinsing steps is required to remove non-adsorbed protein present in the inner part of the scaffolds. [§]In this application, immobilized peptide rather than adsorbed protein was quantified.

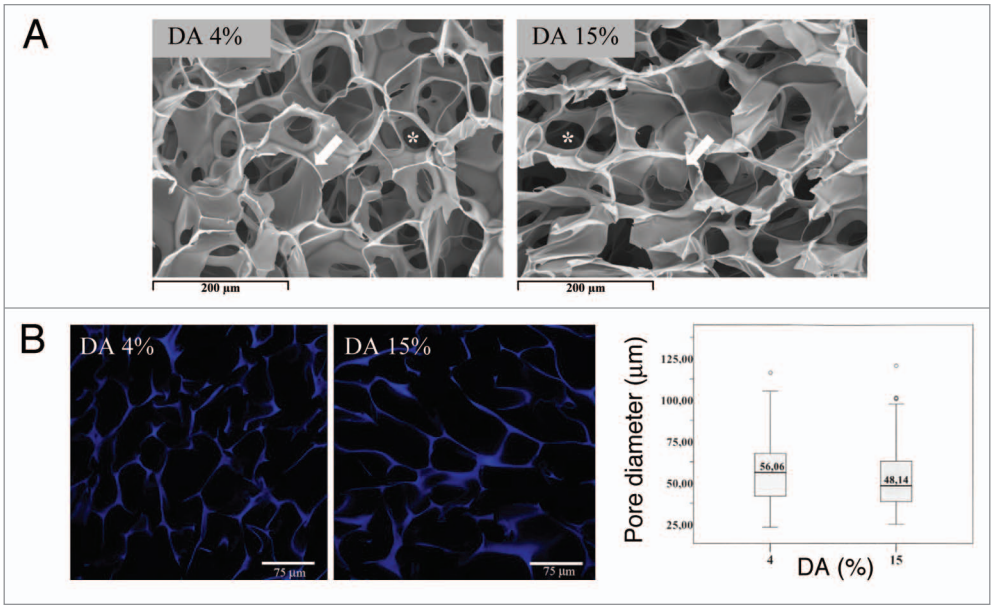

Figure 1. Morphological analysis of CH porous scaffolds with DA 4% and 15%. (**A**) SEM micrographs of transversal cross-sections of the dehydrated scaffolds, showing a highly porous and interconnected structure, with macropores (arrow) and interconnecting pores (*). (**B**) CLSM imaging of 100 µm thick cryosections of hydrated CH scaffolds. The polymeric structure is shown in blue due to CH autofluorescence upon excitation by the 405 nm laser. The pore diameter distribution resultant from image analysis is shown in the box plot chart, and depicts the following statistics: minimum, first quartile, median, third quartile, and maximum. Pinpoints represent outliers. Values reported correspond to 120 measurements made in CLSM images of cryosections obtained from four different CH scaffolds.

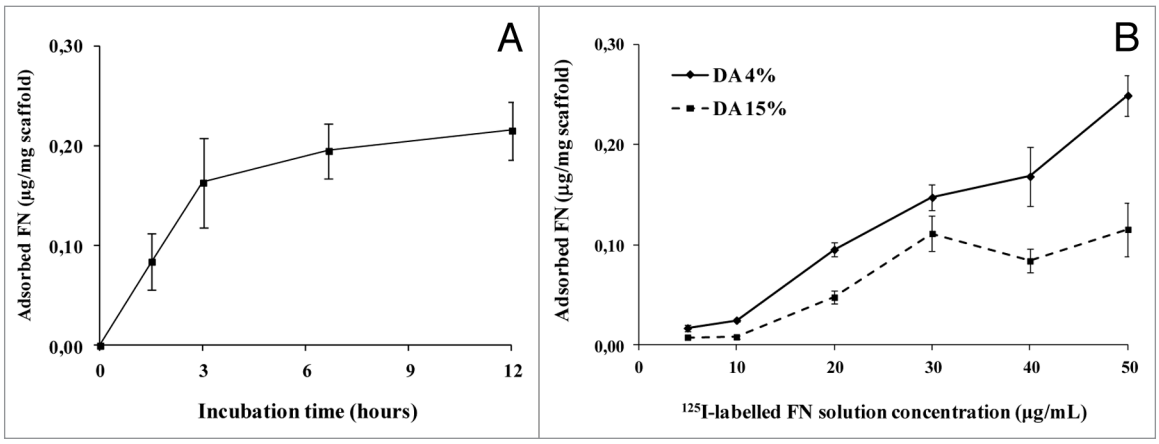

Figure 2. Kinetics and isotherms of FN adsorption to CH scaffolds, as determined using ^{125}I-labeled FN. (**A**) FN adsorption to CH (DA 4%) from a 20 µg/mL FN solution, as a function of incubation time (mean ± SD; n = 8). (**B**) FN adsorption to CH scaffolds (DA 4 and 15%; 15-h incubation period), as a function of FN solution concentration (mean ± SD; n = 6). All the FN levels shown were determined after subsequent incubation of the porous scaffolds in complete culture medium for 24 h.

distribution of FN with exposure of cell-binding domains, which was more evident for DA 4% scaffolds (**Fig. 4A and B**). At higher magnification, small spots with higher fluorescence intensity and possibly corresponding to FN aggregates were also observed, besides a more diffuse coating of FN. To further quantify the exposure of cell-binding domains on FN-coated scaffolds, fluorimetry analysis of cryosections was performed. Results revealed significantly higher (2.6-fold higher, $p < 0.001$) fluorescence intensity values for scaffolds with DA 4% as compared with DA 15%, indicating the exposure of a higher number of integrin-binding domains upon FN adsorption (**Fig. 4C**).

Cell adhesion and cytoskeletal organization of HPMEC-ST1.6R cells on CH scaffolds as a function of FN concentration. Incubation in a FN solution resulted in statistically significantly higher cell numbers as compared with scaffolds merely incubated in CCM, for both the DAs tested (**Fig. 5**). Nevertheless, for the same DA, no positive correlation was found between cell numbers and FN concentration, and no statistically significant

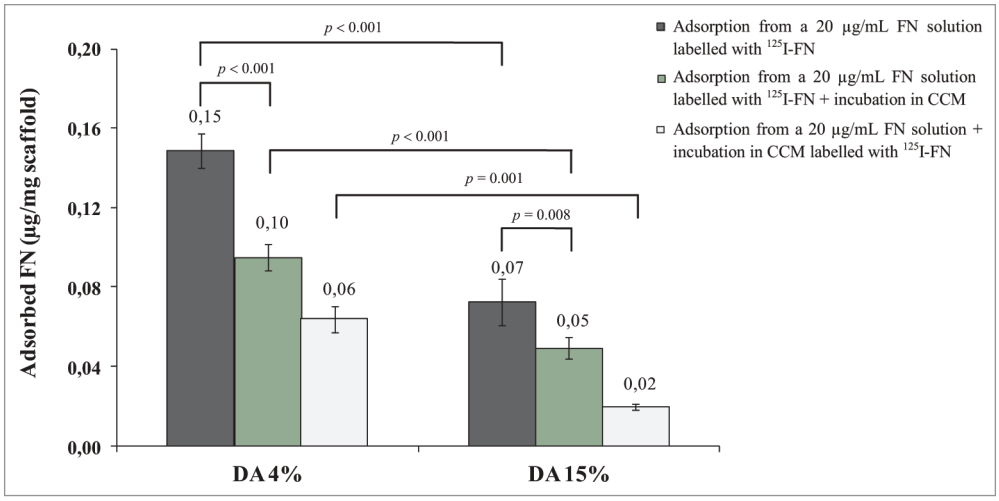

Figure 3. Fibronectin adsorption to CH scaffolds (DA 4 and 15%) from a 20 µg/mL FN solution, as well as elution and exchangeability of pre-adsorbed FN in the presence of serum proteins. FN adsorption levels were determined by gamma counting after a 15-h incubation period in a 20 µg/mL ^{125}I-labeled FN solution. To estimate the elution of pre-adsorbed FN in the presence of serum proteins, samples were further immersed in complete culture medium (CCM) for 24 h, and the levels of remaining FN quantified by gamma counting. The exchangeability of pre-adsorbed FN by new FN molecules from serum was investigated incubating samples pre-adsorbed with unlabelled FN (20 µg/mL) in CCM containing ^{125}I-FN. Results presented are the mean ± SD (n = 6).

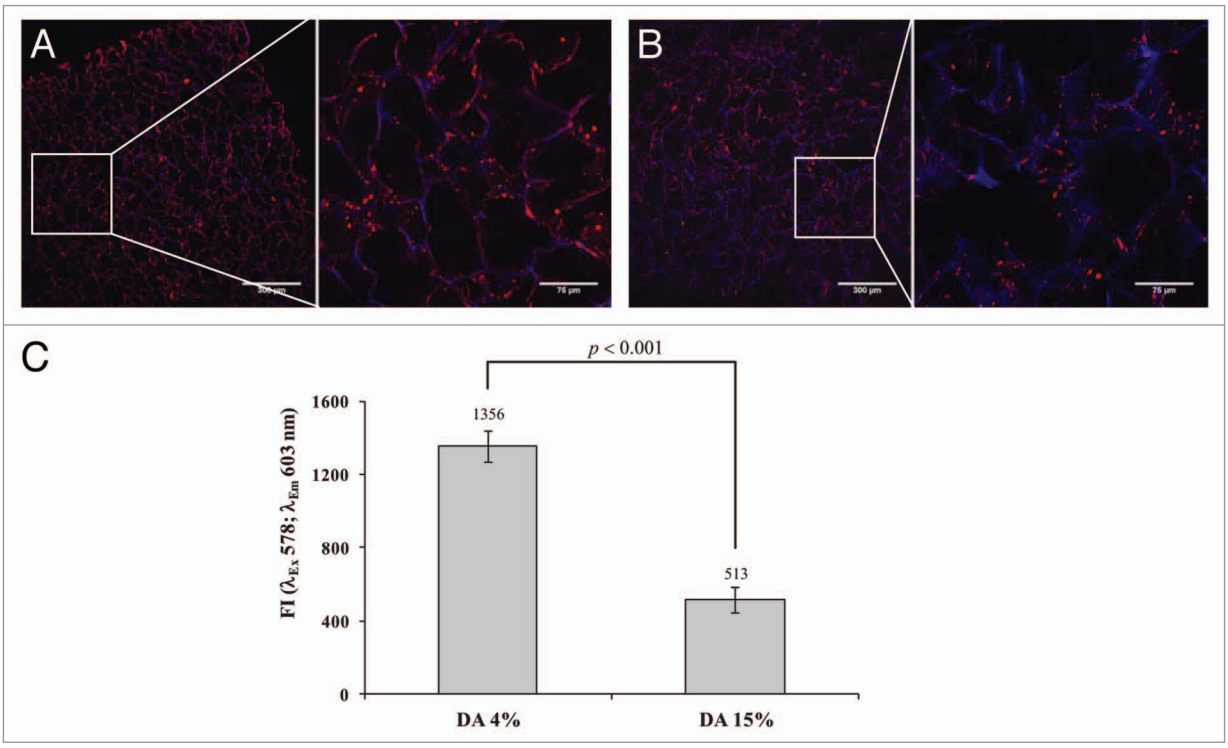

Figure 4. Distribution and conformation of FN upon adsorption to CH scaffolds with DA 4% (**A**) and 15% (**B**), as probed by immunofluorescent staining of the integrin-binding RGD site of FN. Scaffolds were incubated in a 20 µg/mL FN solution for 15 h, cryosectioned, processed for immunofluorescence, and imaged by CLSM. The scale bar for the low- and high-magnification images corresponds to 300 µm and 75 µm, respectively. (**C**) Quantitative analysis of exposed cell-binding domains, as determined by fluorimetry. Results reported are the mean ± SD of fluorescence intensity (FI) values correspondent to 8 cryosections.

differences were found among the different FN solutions used, for the range of FN concentrations tested (from 5 to 50 µg/mL). Regardless of the FN solution concentration used, cell numbers on DA 15% were always lower than those found on DA 4%,

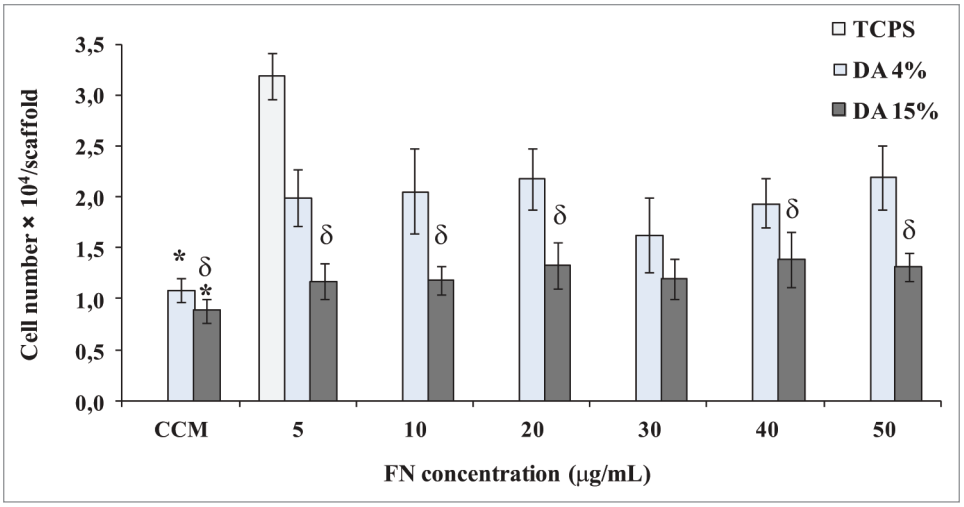

Figure 5. Cell adhesion of HPMEC-ST1.6R cells to CH scaffolds (DA 4 and 15%) previously incubated for 15 h in complete culture medium (CCM) or in FN solutions with concentrations ranging from 5 to 50 μg/mL (mean ± SD; n = 6). TCPS coverslips previously incubated in a 5 μg/mL FN solution were used as 2-D substrate control for EC adhesion. *indicates a significant difference from the corresponding CH samples incubated in FN solutions. $^{\delta}$indicates a significant difference from CH samples with DA 4%, when subjected to the same incubation conditions ($p \leq 0.05$).

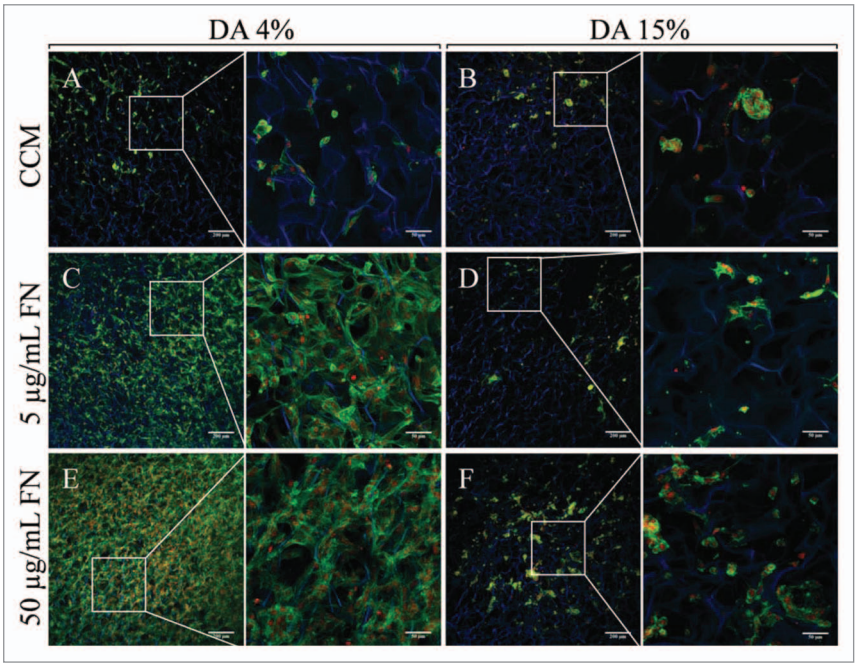

Figure 6. Fluorescent labeling of F-actin (green) and DNA (red) of HPMEC-ST1.6R cells cultured on CH scaffolds (DA 4 and 15%) previously incubated in complete culture medium (**A and B**) or in FN solutions with concentrations of 5 (**C and D**) and 50 μg/mL (**E and F**). Images obtained by CLSM, 144 h after cell seeding (Scale bar: 200 μm and 50 μm the low- and high-magnification images, respectively).

although a statistical significant difference was not achieved in case of incubation in a 30 μg/mL FN solution.

The influence of FN concentration on EC cytoskeleton organization was assessed 144 h after cell seeding. As shown in **Figure 6A and B**, CH scaffolds merely equilibrated in CCM were not able to sustain cell adhesion of ECs, regardless of the DA. In contrast, incubation of DA 4% scaffolds with FN allowed cytoskeletal organization of adherent cells and subsequent scaffold colonization, with no apparent differences being observed between the lowest and the highest FN concentrations tested, namely 5 and 50 μg/mL (**Fig. 6C and E**). At higher magnification, F-actin/DNA labeling revealed the presence of EC layers constituted by cells preferentially oriented along the polymeric pore walls displaying a flattened morphology and a diffuse distribution of F-actin. Occasionally, dense bundles of actin microfilaments were found at the cell periphery and cell-cell boundaries. In the case of DA 15% scaffolds, very few cells were found remaining attached to the scaffolds, regardless of the FN concentration used (**Fig. 6D and F**). Although slightly more cells were found on scaffolds incubated in the 50 μg/mL FN concentration, at higher magnification, most of the cells displayed a round-shaped morphology with poor cytoskeleton organization (**Fig. 6F**).

Discussion

In the present study ^{125}I-radiolabelling was explored to follow the kinetics and isotherm of FN adsorption to CH porous scaffolds, as well as to assess the elution and exchangeability of adsorbed FN in the presence of serum proteins. The amount, distribution, conformation, and exchangeability of FN upon adsorption strongly influence its ability to mediate endothelial (EC) adhesion to biomaterials.[8,11-13] As a result, the information provided by ^{125}I-radiolabelling was complemented by immunofluorescence studies and then correlated with the ability of passively-adsorbed FN to mediate EC adhesion.

To quantify FN adsorption to CH porous scaffolds, several rinsing steps were performed prior to gamma-counting, to remove most of non-adsorbed protein. A compromise between the number of rinses and the presence of minor amounts of non-adsorbed FN was established, as rinses with buffer may also lead to partial desorption of adsorbed protein, namely of that corresponding to loosely bound protein.[14] We subsequently assessed if ^{125}I-labeling of FN did not alter the profile of FN adsorption to CH. This is

an important issue that needs to be assessed prior to the use of radiolabelling to quantify protein adsorption onto polymeric surfaces.[2] The similar levels of adsorbed FN found on CH porous scaffolds using different ratios of labeled to unlabelled FN indicate that the preferential adsorption of ^{125}I-FN or FN did not occur. Kinetic studies were initially performed to determine the incubation time leading to the highest levels of adsorbed FN on CH. Although FN adsorption took place mainly during the first 3 h of incubation, overnight incubation (15 h) was chosen for all the subsequent assays since the levels of adsorbed FN slightly increased with incubation time. The effect of FN concentration on the levels of adsorbed FN was investigated using FN solutions with concentrations in the range of 5 to 50 μg/mL. The isotherm of FN adsorption on DA 4% scaffolds revealed an almost linear increase of FN adsorption with increasing FN concentration, within the range of FN concentrations tested. A well-defined plateau was not detected at high concentrations, as it is usually observed in isotherms of FN adsorption from FN solutions on 2-D surfaces at ≅ 10 μg/mL.[15] This indicates that saturation adsorption levels were not achieved. The absence of a saturation plateau may be related to the higher surface area available for protein adsorption in the porous scaffolds, in comparison with 2-D surfaces. Another phenomenon that may also have contributed to the absence of a saturation plateau is the possible affinity of free FN molecules for the adsorbed ones, as has been suggested by others for FN adsorption on copolymer surfaces.[16] On DA 15% scaffolds, FN adsorption levelled off at ≅ 30 μg/mL, and significantly lower FN amounts were found as compared with DA 4%, for all the FN concentrations tested. These differences were not related to the structural properties, since the two scaffolds revealed a similar microstructure both in the dry and in the hydrated state. Moreover, as the scaffolds with higher surface area available for protein adsorption revealed the lowest amounts of adsorbed FN, it is likely that the different FN adsorption profiles found for the two scaffolds result from differences in surface chemistry. In CH, the presence of free amine groups in the glucosamine units provides a net positive charge at physiological pH.[17] With the increase of the DA, the concentration of methyl groups from acetylated CH monomeric units increases progressively while that of amine groups decreases. Concomitantly, CHs with higher DAs are expected to present lower values of surface charge, as was previously shown for CH films.[18] The effect of different chemical functionalities on FN adsorption and conformation upon adsorption was investigated by Keselowsky et al., using terminally functionalized self-assembled monolayers of alkanethiols on gold.[19] As compared with methyl groups, amine groups were shown to favor FN adsorption as well as that of a recombinant fragment of FN (rhFNIII$_{7-10}$) exposing the FN cell-binding domain.[19,20] Moreover, amine groups induced less conformational changes on FN/rhFNIII$_{7-10}$ upon adsorption as well as higher retention of integrin binding ability and recruitment of focal adhesion components, thus suggesting a lower degree of protein unfolding/denaturation.[21] As a result, the higher levels of adsorbed FN found on DA 4% scaffolds as compared with DA 15% were possibly influenced by the higher amount of amine groups present at the surface. Moreover, amine groups also probably contributed to the higher ability of DA 4% scaffolds to exchange pre-adsorbed FN by other FN molecules present in CCM, as protein adsorption reversibility may be more favorable for proteins that undergo a lesser degree of conformational change upon adsorption.

Immunofluorescent labeling of FN cell-binding domains complemented the quantitative analysis of FN adsorption to CH provided by radiolabelling experiments, namely in terms of conformation and organization of adsorbed FN on CH. CLSM imaging of cryosections of CH scaffolds previously incubated in a 20 μg/mL FN solution showed an homogeneous distribution of FN cell-adhesion domains on both DAs, and allowed the detection of protein aggregation. Subsequent analysis of the cryosections by fluorimetry revealed the presence of a higher amount of exposed FN cell-binding domains on DA 4% as compared with DA 15%, in accordance with FN adsorption results.

The efficacy of passively adsorbed FN to mediate EC adhesion to CH was subsequently assessed. In line with the literature, EC cell adhesion and cytoskeletal organization on CH scaffolds merely incubated in CCM was poor regardless of the DA.[8,22,23] The low levels of adsorbed FN and exposed cell-binding domains found on these matrices may have contributed to CH inability to support EC adhesion and cytoskeletal organization. However, due to the presence of serum in CCM, other proteins besides FN may have also influenced EC behavior on CH. Incubation with FN solutions resulted in significantly higher numbers of adherent cells, for both DAs tested. However, for the same DA, no positive correlation was found between cell numbers and the FN solution concentration. In fact, in the case of DA 4% scaffolds, the lowest FN concentration tested (5 μg/mL) was already efficient in promoting EC adhesion and cytoskeletal reorganization, as well as the formation of EC layers. In contrast, incubation of DA 15% scaffolds with FN typically resulted in lower cell numbers and in cells displaying mostly a spherical-like morphology. The lower levels of adsorbed FN found on DA 15% as compared with DA 4%, possibly contributed to the lower number of adherent cells found on DA 15%. Nevertheless, the inability of DA 15% to support EC adhesion and cytoskeletal organization cannot be uniquely attributed to the low levels of adsorbed FN. In fact, based on the isotherms of FN adsorption to CH, the levels of adsorbed FN found on DA 15% scaffolds following incubation in 20 μg/mL FN solution are superior to those found on DA 4% scaffolds upon incubation in a 5 μg/mL FN solution. As a consequence, substrate-induced conformational changes of adsorbed FN affecting the availability of FN cell-binding epitopes for integrin binding possibly also contributed to the poor EC behavior on DA 15%. The lower reversibility of FN adsorption on these scaffolds suggest, at least to a certain degree, protein unfolding and loss of functional activity. In fact, Renner et al. reported a correlation between FN exchangeability and EC behavior, FN exchangeability leading to enhanced formation of focal adhesions.[13] As a minimum density of FN cell-binding epitopes is required for integrin clustering, focal adhesion assembly, and

Table 2. Chitosan characterization in terms of degree of acetylation (DA), weight- and number-average molecular weight (*Mw* and *Mn*, respectively), polydispersity index (PDI), and endotoxin content

DA (%)	*Mw* × 10^5	*Mn* × 10^5	*PDI*	Endotoxin (EU/g)
3.55 ± 0.32	5.0 ± 0.2	2.7 ± 0.1	1.8. ± 0.1	Not detected[a]
15.35 ± 1.26	4.3 ± 0.1	2.0 ± 0.0	2.2 ± 0.1	Not detected[a]

[a]Endotoxin levels below the minimal detection level of the LAL test used (0.1 EU/mL), a EU corresponding to a unit of measurement for endotoxin activity.

actin polymerization,[24] present results suggest that while a 5 μg/mL FN solution was effective in providing CH with DA 4% with adequate amounts of cell-binding domains, the same was not true for DA 15%, even when using a FN solution concentration as high as 50 μg/mL. Based on these results, strategies to achieve successful endothelialisation of CH porous scaffolds within a wide range of DAs are presently being explored by our group.

Materials and Methods

Chitosan (CH) characterization. Squid pen CH was supplied by France Chitine (Batch n° 171204; DA below 5%), being subsequently purified by filtration of CH acidic solution followed by alkali precipitation. Chitosan with a DA of approximately 15% was prepared by *N*-acetylation using acetic anhydride as reactant in water/acetic acid/1,2-propanediol solution, according to Vachoud L et al.[25] The "as received" and acetylated CH were characterized in terms of DA (Fourier Transform Infrared Spectrometry performed in KBr pellets using the band at 1320 cm^{-1} as the analytical band and the band at 1420 cm^{-1} as the internal reference band),[26] average molecular weight and polydispersity index (high-performance size exclusion chromatography),[27] as well as in terms of endotoxin content (Limulus Amebocyte Lysate test performed in water extracts)[18] (**Table 2**).

Preparation and characterization of 3-D porous scaffolds. Porous scaffolds were prepared from a 2% w/v CH acidic solution via thermally induced phase separation and subsequent sublimation of the ice crystals. Briefly, the polymer was allowed to dissolve in 0.2 M acetic acid for 24 h, poured into the wells of 24-well tissue culture plates (TPP®), frozen at –20°C and then lyophilized for 48 h. The resultant scaffolds were cut transversally (3 × 3 × 2 mm^3) and the attainment of a porous and homogeneous structure confirmed by scanning electron microscopy (SEM). The surface area of the resultant scaffolds was characterized by mercury intrusion porosimetry, using a PoreMaster 60® porosimeter (Quantachrome Instruments). Four scaffolds with a total weight of approximately 0.030 g were used in each measurement. The contact angle of mercury on CH was 140° and mercury surface tension was 480 erg/cm^2. A total of 982 low- and high-pressure intrusion points was collected in the range of 0.042 PSIA to 59,000 PSIA. The microstructure of the scaffolds following sterilization and hydration was also assessed. For this purpose the lyophilized scaffolds were successively immersed in filter sterilized absolute ethanol and diluted ethanol solutions (70, 50, and 25% v/v), under reduced pressure. Finally, the scaffolds were equilibrated (2×) in sterile phosphate-buffered saline (PBS, pH 7.4), cryosectioned transversally at 100 μm, and analyzed by confocal laser scanning microscopy (CLSM). Pore diameter was calculated using the relation:

$$d = \sqrt{l \cdot h}$$

where l and h are the maximum and the minimum pore lengths, respectively.

Fibronectin (FN) adsorption to CH scaffolds. Fibronectin adsorption studies were performed using human plasma FN (Sigma) labeled with ^{125}I (^{125}I-FN). FN was labeled with ^{125}I ($Na^{125}I$, Perkin Elmer) using the Iodogen method,[28] and further purified using a Sephadex™ G-25 Medium column (PD-10 column, Amersham Biosciences), to remove unbound ^{125}I. Fractions with yield of ^{125}I-labeling ≥ 98.5% were used. Labeled protein was stored at –20°C and used within 3 d. Labeled protein solutions were prepared by adding ^{125}I-FN to unlabelled solutions to obtain a final activity of ≅ 3 × 10^6 cpm/mL. Prior to the protein adsorption assays CH scaffolds were individually weighed, sterilized and hydrated as described above, and finally equilibrated overnight in degassed PBS with 0.01 M NaI (PBSI) to prevent adsorption of free ^{125}I ions present in trace amounts in ^{125}I-FN. All incubations steps were performed at 37°C and 250 rpm in a thermostat-regulated orbital shaker, using 50 μL of FN solution per scaffold. To assess if preferential adsorption of ^{125}I-labeled FN or unlabelled FN occurred on CH sponges, a series of control experiments was performed by varying the ratio of labeled to unlabelled FN (2, 4, 10, and 20% v/v). For this purpose each scaffold was incubated in 20 μg/mL ^{125}I-FN labeled FN solutions prepared in degassed PBSI, for 90 min. Before gamma counting, each scaffold was repeatedly rinsed and squeezed in PBS (200 μL; 8×), immersed in PBS for 15 h at RT, rinsed once again in PBS, and finally transferred to radioimmunoassay tubes. The rinsing procedure was optimized in order to remove both free iodine and non-adsorbed protein (**Fig. S4A and S4B**). For gamma activity counting a gamma counter (Wallac Wizard model 1470) was used. The amount of adsorbed FN was determined according to the following equation:

$$FN\ adsorption\ (\mu g/mg\ scaffold) = \frac{Activity_{sample}\ (cpm) \times |FN|_{solution}\ (\mu g/mL)}{Specific\ Activity_{solution}\ (cpm/mL) \times scaffold\ weight\ (mg)}$$

where $Activity_{sample}$ is the gamma activity of the sample expressed in counts per minute (cpm), $Specific\ Activity_{solution}$ is the gamma activity of the FN solution expressed in counts per mL of solution, and |FN| is the concentration of the FN solution. The kinetics of FN adsorption to CH was followed incubating the scaffolds in a 20 μg/mL FN solution for different time periods, up to 12 h. The adsorption isotherm of FN was determined by incubating the scaffolds in ^{125}I-FN labeled FN solutions with concentrations of 5, 10, 20, 30, 40 and 50 μg/mL for 15 h (overnight). In both kinetic and isotherm studies, the samples were further incubated in 200 μL of complete culture medium (CCM) containing 20% (v/v) fetal bovine serum for 24 h before being processed for gamma counting (Details of CCM composition are given in supporting data). Finally, to assess the ability of bare CH scaffolds to adsorb FN molecules from CCM, samples were incubated in CCM labeled with ^{125}I-FN for 15 h.

Elution and exchangeability of adsorbed FN upon incubation in complete culture medium (CCM). The elution and the exchangeability of pre-adsorbed FN in the presence of serum proteins were determined in CH matrices previously incubated in a 20 μg/mL FN solution for 15 h. The initial FN adsorption levels were quantified as described above, using ^{125}I-labeled FN (20 μg/mL). To estimate the elution of pre-adsorbed FN, samples incubated with ^{125}I-labeled FN (20 μg/mL) were further immersed in CCM for 24 h, and the levels of remaining FN quantified by gamma counting. The exchangeability of pre-adsorbed FN by new FN molecules from serum was investigated by incubating samples previously adsorbed with unlabelled FN (20 μg/mL) with CCM containing ^{125}I-FN.

Immunofluorescence analysis of fibronectin (FN) exposure of cell-binding domains. The exposure of FN cell-binding domains upon adsorption from a FN solution or from CCM was assessed by immunofluorescence, using three scaffolds per condition. Scaffolds were incubated in a 20 μg/mL FN solution in PBS or in CCM for 15 h at 37°C and 250 rpm, as described above. Following incubation, scaffolds were rinsed with PBS (3×), flash frozen in liquid nitrogen and cryosectioned, resulting in 100 μm thick transversal crossections. Cryosections corresponding to the central part of each scaffold were processed for immunofluorescence. Samples incubated in buffer (PBS) without protein were also processed to provide controls for nonspecific antibody binding. All subsequent incubation steps were performed at 37°C and 50 rpm, during 1 h. Briefly, samples were incubated in a 1% heat-denatured bovine serum albumin (BSA) solution in PBS for 1 h, washed with PBS, and then incubated with the primary antibody diluted 1:1000 in blocking buffer (0.25% BSA, 0.05% Tween-20 in PBS). Mouse anti-human monoclonal antibody HFN 7.1 (Developmental Studies Hybridoma Bank) was used for samples incubated with FN. This antibody binds to the major integrin-binding RGD site of human FN, and has proved to be an effective probe to measure FN functionality following adsorption onto different substrates.[19] For scaffolds incubated with CCM, a mouse anti-bovine FN monoclonal antibody directed against the cell-binding fragment of FN (CSI 005–17, AntibodyShop) was used. After washing with blocking buffer, samples were incubated with Alexa Fluor 568-conjugated goat anti-mouse IgG (Molecular Probes) diluted in blocking buffer at 5 μg/mL, rinsed, mounted with Fluoromount (Sigma) and immediately observed under CLSM. Fluorescence intensity (FI) was quantified by fluorimetry. For that purpose, each cryosection was transferred to a well of a 24-well TCPS plate, and the corresponding FI read (λ_{Ex} 578 nm; λ_{Em} 603 nm) using a BioTek® Synergy™ MX plate reader with the optics position set to bottom. The FI values were determined by subtracting the average FI value of the correspondent control.

Cell culture. A cell line of human pulmonary microvascular endothelial cells (HPMEC-ST1.6R cell line) displaying most of the major constitutively expressed and inducible endothelial phenotypic markers was used.[29,30] Details of HPMEC-ST1.6R cell culture are given in supporting data.

Cell seeding on the 3-D scaffolds. Prior to cell seeding CH scaffolds were sterilized and hydrated as described above, and then incubated overnight (15 h) either in CCM or in FN solutions with concentrations ranging from 5 to 50 μg/mL. Incubation was performed at 37°C and 250 rpm, as described above. Finally, the scaffolds were transferred to the wells of a 96-well tissue culture plate and seeded with 9 μL of a cell suspension prepared at 3 × 10^6 cells/mL in CCM (2.7 × 10^4 cells/scaffold). Scaffolds were incubated at 37°C for 4 h to allow for initial cell attachment, after which 200 μL of CCM were added. Finally, the seeded scaffolds were transferred to the incubator, and cultured for 24 h. Fibronectin-coated wells (400 μL of a 5 μg/mL FN solution in PBS) seeded in parallel with the same volume of cell suspension were used as 2-D substrate control for EC adhesion.

Cell adhesion. Cell adhesion to CH scaffolds was inferred from cell metabolic activity determined 24 h after cell seeding using a resazurin-based assay, as previously described.[8] Fluorescence was measured (λ_{Ex} 530 nm; λ_{Em} 590 nm) and the fluorescence value correspondent to unseeded scaffolds subtracted. Cell number was extrapolated from a standard curve in which fluorescence was plotted against known number of HPMECs seeded in parallel on FN-coated wells and further incubated during 3 h to allow for cell adhesion.

Cytoskeletal organization. Cytoskeleton organization was assessed 144 h after cell seeding. Briefly, the cells were rinsed twice with PBS, fixed in 3.7% paraformaldehyde, permeabilized in 0.2% (v/v) buffered Triton X-100 for 10 min, and incubated with 1% w/v BSA/PBS for 1 h. Cell cytoskeletal filamentous actin (F-actin) was visualized by treating the cells with 5 U/mL Alexa Fluor 488 phalloidin (Molecular Probes) in 1% BSA/PBS for 60 min. Cell nuclei were counterstained with propidium iodide (Sigma) diluted in PBS (15 μM) for 10 min. Samples were finally mounted with Fluoromount (Sigma) and immediately observed under CLSM.

Statistical analysis. Sample distribution was tested for normality using the Kolmogorov–Smirnov test, and data subsequently analyzed using the unpaired t-test. A 95% confidence level was considered statistically significant. Calculations were performed using IBM® SPSS® Statistics (version 19).

Conclusions

In this study, ^{125}I-radiolabelling was successfully used to establish the kinetics and isotherm of FN adsorption onto chitosan porous scaffolds, as well as on the elution and exchangeability of pre-adsorbed FN in the presence of serum-containing medium. The results showed that the isotherm of FN adsorption is DA dependent, DA 4% scaffolds adsorbing higher FN amounts as compared with DA 15% scaffolds, independently of the FN concentration tested. These findings were further supported by immunofluorescent studies in cryosections which revealed, for the same FN concentration, higher number of exposed FN cell-binding domains on DA 4% as compared with DA 15%. In line with the higher FN adsorption levels found, when assessing the efficacy of passively adsorbed FN in promoting EC adhesion and cytoskeletal reorganization on CH, ECs were found to adhere at

higher levels to DA 4% as compared with DA 15%, 5 μg/mL of FN being already efficient in mediating cell adhesion and cytoskeletal organization on CH with DA 4%.

The present study shows that radiolabelling is a powerful tool to study protein adsorption to porous polymeric scaffolds under physiological conditions, complementing the currently available methods used to dissect cell-material interactions.

Disclosure of Potential Conflicts of Interest

No potential conflicts of interest were disclosed.

Acknowledgments

This work was financed by FEDER funds through the Programa Operacional Factores de Competitividade—COMPETE and by Portuguese funds through FCT—Fundação para a Ciência e a Tecnologia in the framework of the project PEst-C/SAU/LA0002/2011 and PTDC/SAU-BEB/65328/2006).

Supplemental Materials

Supplemental materials may be found here:
www.landesbioscience.com/journals/biomatter/article/24791

References

1. Ratner BD, Hoffman AS, Schoen FJ, Lemons JE, eds. Biomaterials science: an introduction to materials in medicine. San Diego: Elsevier Academic Press, 2004.
2. Chinn JA, Slack SM. Biomaterials: Protein Surface Interactions. In: Bronzino JD, ed. The Biomedical Engineering Handbook. Boca Raton: CRC Press LLC, 2000:1597-608.
3. Dee KC, Puleo DA, Bizios R. Protein-Surface Interactions. In: Dee KC, Puleo DA, Bizios R, eds. An Introduction To Tissue-Biomaterial Interactions. New York, USA: John Wiley & Sons, Inc, 2003:37-52.
4. Sousa SR, Moradas-Ferreira P, Saramago B, Melo LV, Barbosa MA. Human serum albumin adsorption on TiO2 from single protein solutions and from plasma. Langmuir 2004; 20:9745-54; PMID:15491210; http://dx.doi.org/10.1021/la049158d.
5. González-García C, Sousa SR, Moratal D, Rico P, Salmerón-Sánchez M. Effect of nanoscale topography on fibronectin adsorption, focal adhesion size and matrix organisation. Colloids Surf B Biointerfaces 2010; 77:181-90; PMID:20185279; http://dx.doi.org/10.1016/j.colsurfb.2010.01.021.
6. Gonçalves IC, Martins MCL, Barbosa MA, Ratner BD. Protein adsorption and clotting time of pHEMA hydrogels modified with C18 ligands to adsorb albumin selectively and reversibly. Biomaterials 2009; 30:5541-51; PMID:19595453; http://dx.doi.org/10.1016/j.biomaterials.2009.06.025.
7. Barrias CC, Martins MCL, Almeida-Porada G, Barbosa MA, Granja PL. The correlation between the adsorption of adhesive proteins and cell behaviour on hydroxyl-methyl mixed self-assembled monolayers. Biomaterials 2009; 30:307-16; PMID:18952279; http://dx.doi.org/10.1016/j.biomaterials.2008.09.048.
8. Amaral IF, Unger RE, Fuchs S, Mendonça AM, Sousa SR, Barbosa MA, et al. Fibronectin-mediated endothelialisation of chitosan porous matrices. Biomaterials 2009; 30:5465-75; PMID:19615736; http://dx.doi.org/10.1016/j.biomaterials.2009.06.056.
9. Tomihata K, Ikada Y. In vitro and in vivo degradation of films of chitin and its deacetylated derivatives. Biomaterials 1997; 18:567-75; PMID:9105597; http://dx.doi.org/10.1016/S0142-9612(96)00167-6.
10. Slack M. Properties of Biological Fluids. In: Ratner BD, Hoffman AS, Schoen FJ, Lemons JE, eds. Biomaterials Science - An Introduction to Materials in Medicine. Amsterdam: Elsevier, 2004:813-7.
11. Tidwell CD, Ertel SI, Ratner BD, Tarasevich BJ, Atre S, Allara DL. Endothelial cell growth and protein adsorption on terminally functionalized, self-assembled monolayers of alkanethiolates on gold. Langmuir 1997; 13:3404-13; http://dx.doi.org/10.1021/la9604341.
12. Koenig AL, Gambillara V, Grainger DW. Correlating fibronectin adsorption with endothelial cell adhesion and signaling on polymer substrates. J Biomed Mater Res A 2003; 64:20-37; PMID:12483693; http://dx.doi.org/10.1002/jbm.a.10316.
13. Renner L, Jørgensen B, Markowski M, Salchert K, Werner C, Pompe T. Control of fibronectin displacement on polymer substrates to influence endothelial cell behaviour. J Mater Sci Mater Med 2004; 15:387-90; PMID:15332604; http://dx.doi.org/10.1023/B:JMSM.0000021107.12809.8d.
14. Leibner ES, Barnthip N, Chen WN, Baumrucker CR, Badding JV, Pishko M, et al. Superhydrophobic effect on the adsorption of human serum albumin. Acta Biomater 2009; 5:1389-98; PMID:19135420; http://dx.doi.org/10.1016/j.actbio.2008.11.003.
15. García AJ, Vega MD, Boettiger D. Modulation of cell proliferation and differentiation through substrate-dependent changes in fibronectin conformation. Mol Biol Cell 1999; 10:785-98; PMID:10069818.
16. Kowalczynska HM, Nowak-Wyrzykowska M, Kołos R, Dobkowski J, Kaminski J. Fibronectin adsorption and arrangement on copolymer surfaces and their significance in cell adhesion. J Biomed Mater Res A 2005; 72:228-36; PMID:15625681; http://dx.doi.org/10.1002/jbm.a.30238.
17. Denuziere A, Ferrier D, Damour O, Domard A. Chitosan-chondroitin sulfate and chitosan-hyaluronate polyelectrolyte complexes: biological properties. Biomaterials 1998; 19:1275-85; PMID:9720891; http://dx.doi.org/10.1016/S0142-9612(98)00036-2.
18. Amaral IF, Cordeiro AL, Sampaio P, Barbosa MA. Attachment, spreading and short-term proliferation of human osteoblastic cells cultured on chitosan films with different degrees of acetylation. J Biomater Sci Polym Ed 2007; 18:469-85; PMID:17540120; http://dx.doi.org/10.1163/156856207780425068.
19. Keselowsky BG, Collard DM, García AJ. Surface chemistry modulates fibronectin conformation and directs integrin binding and specificity to control cell adhesion. J Biomed Mater Res A 2003; 66:247-59; PMID:12888994; http://dx.doi.org/10.1002/jbm.a.10537.
20. Michael KE, Vernekar VN, Keselowsky BG, Meredith JC, Latour RA, Garcia AJ. Adsorption-induced conformational changes in fibronectin due to interactions with well-defined surface chemistries. Langmuir 2003; 19:8033-40; http://dx.doi.org/10.1021/la034810a.
21. Keselowsky BG, Collard DM, García AJ. Surface chemistry modulates focal adhesion composition and signaling through changes in integrin binding. Biomaterials 2004; 25:5947-54; PMID:15183609; http://dx.doi.org/10.1016/j.biomaterials.2004.01.062.
22. Chung TW, Lu YF, Wang SS, Lin YS, Chu SH. Growth of human endothelial cells on photochemically grafted Gly-Arg-Gly-Asp (GRGD) chitosans. Biomaterials 2002; 23:4803-9; PMID:12361619; http://dx.doi.org/10.1016/S0142-9612(02)00231-4.
23. Cuy JL, Beckstead BL, Brown CD, Hoffman AS, Giachelli CM. Adhesive protein interactions with chitosan: consequences for valve endothelial cell growth on tissue-engineering materials. J Biomed Mater Res A 2003; 67:538-47; PMID:14566796; http://dx.doi.org/10.1002/jbm.a.10095.
24. Coussen F, Choquet D, Sheetz MP, Erickson HP. Trimers of the fibronectin cell adhesion domain localize to actin filament bundles and undergo rearward translocation. J Cell Sci 2002; 115:2581-90; PMID:12045228.
25. Vachoud L, Zydowicz N, Domard A. Formation and characterisation of a physical chitin gel. Carbohydr Res 1997; 302:169-77; http://dx.doi.org/10.1016/S0008-6215(97)00126-2.
26. Brugnerotto J, Lizardi J, Goycoolea FM, Arguelles-Monal W, Desbrieres J, Rinaudo M. An infrared investigation in relation with chitin and chitosan characterization. Polymer (Guildf) 2001; 42:3569-80; http://dx.doi.org/10.1016/S0032-3861(00)00713-8.
27. Terbojevich M, Cosani A, Muzzarelli RAA. Molecular parameters of chitosans depolymerized with the aid of papain. Carbohydr Polym 1996; 29:63-8; http://dx.doi.org/10.1016/0144-8617(95)00147-6.
28. Iodine-125, a guide to radioiodination techniques. Little Chalfont, Buckinghamshire, UK: Amersham International, 1993.
29. Krump-Konvalinkova V, Bittinger F, Unger RE, Peters K, Lehr HA, Kirkpatrick CJ. Generation of human pulmonary microvascular endothelial cell lines. Lab Invest 2001; 81:1717-27; PMID:11742042; http://dx.doi.org/10.1038/labinvest.3780385.
30. Unger RE, Krump-Konvalinkova V, Peters K, Kirkpatrick CJ. In vitro expression of the endothelial phenotype: comparative study of primary isolated cells and cell lines, including the novel cell line HPMEC-ST1.6R. Microvasc Res 2002; 64:384-97; PMID:12453433; http://dx.doi.org/10.1006/mvre.2002.2434.
31. Bajpai AK, Mishra DD. Adsorption of fibrinogen onto macroporous, biocompatible sponges based on poly(2-hydroxyethyl methacrylate). J Appl Polym Sci 2006; 102:1341-55; http://dx.doi.org/10.1002/app.24127.
32. Bajpai AK. Fibrinogen adsorption onto macroporous polymeric surfaces: correlation with biocompatibility aspects. J Mater Sci Mater Med 2008; 19:343-57; PMID:17597372; http://dx.doi.org/10.1007/s10856-006-0024-y.
33. Chen Y, Feng B, Zhu Y, Weng J, Wang J, Lu X. Preparation and characterization of a novel porous titanium scaffold with 3D hierarchical porous structures. J Mater Sci Mater Med 2011; 22:839-44; PMID:21431352; http://dx.doi.org/10.1007/s10856-011-4280-0.
34. Woo KM, Chen VJ, Ma PX. Nano-fibrous scaffolding architecture selectively enhances protein adsorption contributing to cell attachment. J Biomed Mater Res A 2003; 67:531-7; PMID:14566795; http://dx.doi.org/10.1002/jbm.a.10098.
35. Leong MF, Chian KS, Mhaisalkar PS, Ong WF, Ratner BD. Effect of electrospun poly(D,L-lactide) fibrous scaffold with nanoporous surface on attachment of porcine esophageal epithelial cells and protein adsorption. J Biomed Mater Res A 2009; 89:1040-8; PMID:18478557; http://dx.doi.org/10.1002/jbm.a.32061.

36. Grafahrend D, Calvet JL, Klinkhammer K, Salber J, Dalton PD, Möller M, et al. Control of protein adsorption on functionalized electrospun fibers. Biotechnol Bioeng 2008; 101:609-21; PMID:18461606; http://dx.doi.org/10.1002/bit.21928.
37. Grafahrend D, Heffels KH, Beer MV, Gasteier P, Möller M, Boehm G, et al. Degradable polyester scaffolds with controlled surface chemistry combining minimal protein adsorption with specific bioactivation. Nat Mater 2011; 10:67-73; PMID:21151163; http://dx.doi.org/10.1038/nmat2904.
38. Ho MH, Wang DM, Hsieh HJ, Liu HC, Hsien TY, Lai JY, et al. Preparation and characterization of RGD-immobilized chitosan scaffolds. Biomaterials 2005; 26:3197-206; PMID:15603814; http://dx.doi.org/10.1016/j.biomaterials.2004.08.032.
39. Choi YJ, Choung SK, Hong CM, Shin IS, Park SN, Hong SH, et al. Evaluations of blood compatibility via protein adsorption treatment of the vascular scaffold surfaces fabricated with polylactide and surface-modified expanded polytetrafluoroethylene for tissue engineering applications. J Biomed Mater Res A 2005; 75:824-31; PMID:16138323; http://dx.doi.org/10.1002/jbm.a.30468.